Accuracy Assessment of the Eulerian Two-phase Model for the CFD Simulation of Gas Bubbles Dynamics in Alkaline Electrolyzers

Accuracy Assessment of the Eulerian Two-phase Model for the CFD Simulation of Gas Bubbles Dynamics in Alkaline Electrolyzers

M Dreoni, F Balduzzi, G Ferrara and A Bianchini

Department of Industrial Engineering, Università degli Studi di Firenze, Via di Santa Marta 3, 50139, Firenze, Italy.

Corresponding author: francesco.balduzzi@unifi.it

Abstract. To date, the most industrially developed technology to produce green hydrogen is represented by alkaline water electrolysis (AWE). To improve on design and efficiency of these devices, however, multiphysics simulations based on Computational Fluid Dynamics (CFD) are needed, able to account for electrophysical phenomena and multiphase flows. Focusing on internal flow optimization, the requirements for CFD simulations are anyhow extremely challenging, since solving the gas bubbles' motion implies the solution of a two-phase flow characterized by very low Reynolds numbers and a high fraction of dispersed gas. Despite some interesting studies have been presented in the literature so far, validation of CFD results with detailed experimental measurements is quite rare and, therefore, the reliability of the adopted modelling approaches is not assessed yet. This study presents the results of a multivariate CFD analysis of an electrochemical cell and its validation through a literature test case. Bubbles generation is introduced as a source term, thus overlooking for the moment the electrochemistry to focus on fluid-dynamics. In particular, attention is given to the Eulerian multiphase modelling, investigating the influence of both the inter-phase interaction sub-models' settings (e.g., lift and drag forces, virtual-mass force) and the general settings of the simulation. The mean velocity field of the PIV-measured bubbles is considered to assess the accuracy of numerical predictions, while the available high-definition flow pictures allow a qualitative assessment of the bubbles size and location. CFD results are shown to be in decent agreement with experimental data and able to reproduce the key flow features such as the spreading of the bubble curtains and the gas shifting towards the inner part of the cell. The effect of the bubbles' diameter and of source layer thickness is also discussed.

Keywords: CFD, Electrolyzers, Biphasic Flow, Green Hydrogen, Alkaline

1. Introduction and scope of the study

In recent years hydrogen is experiencing a renewed interest in the scientific community. It has the characteristics to be the energy carrier of the decades to come and its role in the energy sector is pivotal. In fact, it is an alternative way to store the energy coming from renewable plants [1], producing it through electrolysis and then using it in fuel cells, where the only emission is water. In this perspective, it can be somehow classified also as a clean fuel. However, water electrolysis still contributes to a small share of hydrogen production (≈ 4%) [2], despite being a mature technology.

A present challenge to expand the production of green hydrogen is to increase the performance and overall efficiency of electrolyzers. Among the existing types of this device, alkaline water ones are highly developed technologies in the industry. In this case, the basic electrochemical cell has two electrodes (anode and cathode) immersed in a liquid solution of water and electrolytes, as potassium hydroxide (KOH) or sodium hydroxide (NaOH), in a percentage of 20÷40%. Hydroxide ions (OH^-) are transported through the electrolyte solution from the cathode to the anode; hydrogen bubbles are generated at the cathode, whereas oxygen is produced at the anode [3].

The hydrodynamics of the biphasic flow, and in particular the bubbles motion, is closely linked to the overall efficiency of the cell and a thorough study of the bubble dynamics is crucial to allow us a future increase in the cell performance. The presence of bubbles has both positive and negative aspects: on one side, bubbles locally generate turbulence, thus effectively mixing the electrochemical species, while on the other hand they act as insulators on the electrodes, reducing the active surface area. A closer look at the phenomenon, as in [4], shows that bubbles move upward along the vertical electrodes, forming a curtain of increasing width and enhancing the convective transport and the recirculation inside the cell. Common optical techniques generally fail to capture some key features of the biphasic flow, due to the high gas fraction. Therefore, Computational Fluid Dynamics (CFD) is widely used to analyse the complexity of the multiphase flow. However, there is still no consensus on the most suitable CFD models and methods to simulate the cell hydrodynamics, particularly because validation of numerical results with equivalent experimental data is rare.

In this paper a numerical analysis is conducted and a case study from the literature is used to validate the CFD results. The current activity aims at providing a sensitivity analysis on the models and sub-models existing in ANSYS® Fluent® 2020 R2 for the CFD simulation of an electrochemical cell. Furthermore, the influence of bubbles diameter is discussed. The paper is divided into five main sections. After a first brief literature review of the CFD models generally employed, the second section presents the case study, with insight about its configuration and materials. The third section is dedicated to showing the numerical model setup, from geometry and mesh construction to the models and forces considered, among the possibilities offered by Fluent®. Finally, the last two sections present the results and the conclusions.

2. State-of-the-art

The choice of the multiphase settings, sub-models and interfacial forces is crucial to ensure the accuracy of a CFD approach for such complex applications as alkaline electrolyzers.

Concerning the fluid-dynamics model to be employed in case of biphasic flow liquid-gas, two are the main ones used in the literature, i.e., Euler-Euler and Euler-Lagrange. The former describes both phases with transport equations on a globally fixed coordinate system and the notion of volume fraction for each phase is introduced. The latter considers the electrolyte solution as a continuum phase and the bubbles as a discrete phase. In particular, the continuous phase is treated by solving the time-averaged Navier-Stokes equations, whereas Newton equation of motion is solved for each particle of the dispersed phase individually by tracking the particles.

Within the present study, a review of the state-of-the-art of multiphase models' choice for the simulation of electrolyzers biphasic flow was first carried out by the authors. Through investigation of the literature, a few recent CFD works were identified, with different numerical approaches. In most of the analysed papers, a Euler-Euler model was used, with various flow conditions: on one side, a laminar model was employed by Le Bideau et al. [5] and Abdelouahed et al. [6]; on the other side, a turbulent regime was considered by Zarghami et al. [7], using Reynolds Stress Equations (RSE), and by El-Askary [8], who employed a k-ε (STD) model, as recommended by Mat et al. in [9]. A turbulent, or bubble, dispersion force was introduced by most of the cited authors to account for the diffusion of the gas inside the cell, apart from Abdelouahed et al. [6], who considered a negative lift coefficient. Finally, a Euler-Lagrange model was used by Hreiz et al. [4], differently from the above-mentioned papers, with introduction of bubbles at injection points using the Dispersed Phase Model (DPM). In that case, the flow regime was set as laminar and no dispersion forces were employed.

In conclusion, a well-assessed methodology has not been developed yet, due to the novelty of the topic. Therefore, further studies are necessary to assess accuracy and predictive capabilities of multiphase models for this specific application.

3. Case study

The test case analysed for the present study was taken from Hreiz et al. [4], where the two-phase flow hydrodynamics in Vertical Plane Electrode Reactors with Gas Electrogeneration (VPERGEs) is studied and an experimental investigation is carried out. A CFD study was also conducted in the cited paper. The reactor has a No Net Flow Configuration (NNFC) and the free surface of the liquid at the top prevents occurrence of an overall liquid flow in the cell. Hence, the electrolyte solution is transported by the generation and rising of bubbles at the electrodes: it is dragged upward by the gas and moves downward in the central part of the cell, forming two recirculation loops (Figure 1).

In this specific case, the right and left plates are two anodes, and the gas is only composed of oxygen bubbles. The electrolyte is a 0.5 M NaOH aqueous solution in deionised water. The temperature of the cell was kept at 20°C during the experimental campaign. The two anodes' supports are placed at a distance of 6 mm, thus forming a narrow gap, and the overall submerged portion has a depth of 58 mm. The nickel anodes are 30 mm wide and 38 mm high and they are glued to the supports at a 10 mm depth from the free surface (Figure 1).

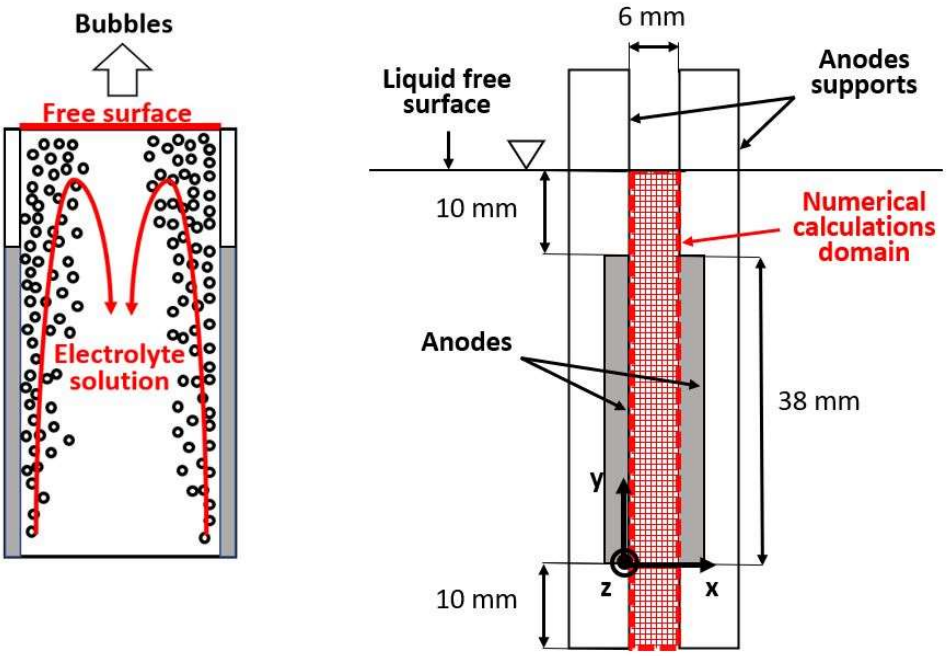

Figure 1. No Net Flow Configuration (NNFC) of the electrochemical reactor and cell geometry

Three average current densities are applied at the anodes, namely 65, 130 and 260 Am^{-2}. The choice of such a reactor instead of a classical electrolysis cell was driven by the fact that it was one of the only and best cases where a good visualization of the bubbles was present. Furthermore, in the cited paper a PIV algorithm was used to find the mean velocity field of the gas, which was used as a reference to validate the numerical model.

Table 1 describes the main properties of the aqueous solution and of the oxygen, respectively the primary and secondary phase, as implemented inside the software program, according to the values in [4]:

Table 1. Material properties.

Materials	Density [kg/m^3]	Viscosity [kg/m s]
Electrolyte solution	1020	1.10e-3
Oxygen	1.30	1.91e-5

4. Numerical model setup

4.1. Geometry and mesh

The numerical modelling of the cell was conducted with ANSYS® 2020 R2 and the fluid-dynamics simulations were performed in Fluent®. The geometry was built using Design Modeler®, coherently with the study-case numerical domain: cell height of 38 mm and a 10 mm outlet. The bottom part of the domain has been extended 10 mm below the anodes segments to enhance stability.

A hexahedral mesh was then built. Due to the small size of bubbles (0.1 mm), the element size of the mesh was chosen to be 0.15 mm, refined at the near-wall regions to simulate more accurately the steep gradient in those areas. A grid independence study showed that a small width of the cells (up to 20 μm at the walls) did not influence the numerical results. Such a study is crucial for numerical analysis to obtain a grid-independent solution. In our case, the mesh has been refined until there was no difference between two consequent solutions and the final mesh reached a total of about 10^6 elements.

4.2. Choice of fluid-dynamic model

Concerning the two main multiphase approaches, Euler-Lagrange and Euler-Euler, the first one is appropriate only for conditions of low gas volume fraction (VF). Since in the present case the VF reaches high values close to the walls [4], a Euler-Euler approach was considered more suitable.

Three different multiphase models are present inside Fluent® for the chosen approach:

1. The Volume Of Fluid (VOF) model, which tracks the surface between phases and considers a unique set of momentum equations, shared by the fluids;
2. The Mixture model, which solves the mixture momentum equations and prescribes relative velocities to describe the dispersed phase;
3. The Eulerian model, which solves a set of conservation equations for each phase, while a single pressure is shared by the phases.

Due to the dispersed condition of bubbles, the third model was employed. The choice of the Eulerian model is validated by the fact that no coalescence may occur inside the cell, as the visualization of the flow in [4] suggests (Figure 2), so that the VOF model was excluded. In fact, bubble coalescence takes place only in the vicinity of the electrodes during the detachment from the surface.

4.3. Model assumptions and boundary conditions

The following hypothesis were considered in the development of the model:

- The pressure is uniform and equal to atmospheric pressure for both phases.
- The flow is Newtonian, incompressible and viscous.
- The cell is assumed to be isothermal, with temperature T=20°C, according to the experimental setup [4].
- The flow is laminar due to the low flow velocities and small pressure gradients;
- The current density distribution is taken as uniform.
- The bubbles dimension is considered constant, thus omitting the non-uniformity of the diameters.
- There is no coalescence inside the cell and the size of oxygen bubbles remains small.

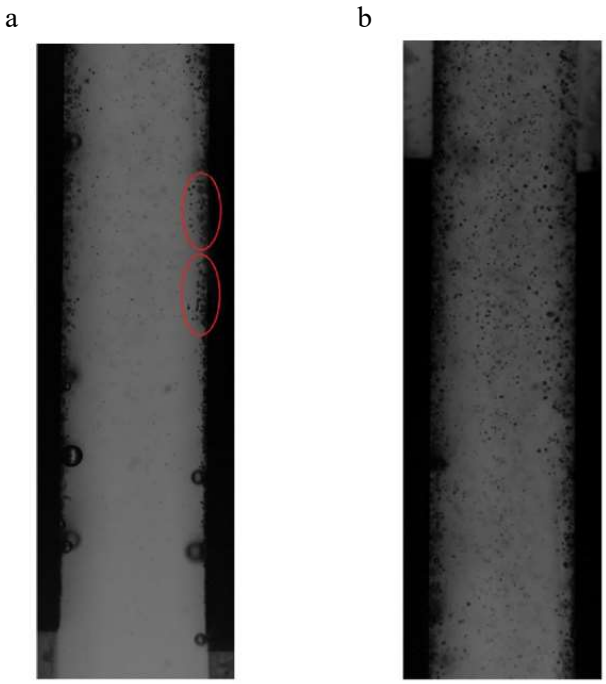

Figure 2. Instantaneous flow field in the case of 130 Am^{-2} current density on the anodes. (a) Lower part of the cell (some bubble clusters are surrounded by red circles). (b) Upper part of the cell [4]

Concerning the boundary conditions, a stationary no-slip wall was set at the anodes and a degassing condition was used as outlet, as recommended in [6]. The last boundary condition considers the outlet boundary as a free surface through which the dispersed gas phase can exit, whereas a zero mass-flow condition is imposed to the primary liquid phase. No inlet boundary was defined since the gas bubbles enter the computational domain through the imposition of a distributed source.

4.4. Source term and bubbles dimension

The bubbles were introduced as a mass source term inside two narrow mesh regions, defined as two near-wall layers of 0.4 mm of thickness in correspondence with anodes. To calculate the amount of oxygen produced we must recall the basic chemistry of electrolysis. The electrochemical reactions involved are the following [10]:

Cathode: $$2H_2O_{(l)} + 2e^- \rightarrow H_{2\,(g)} + 2OH^-_{(aq)} \quad (1)$$

Anode: $$2OH^-_{(aq)} \rightarrow \frac{1}{2}O_{2\,(g)} + H_2O_{(l)} + 2e^- \quad (2)$$

The Faraday's Law was employed [11] to calculate the source-term mass:

$$F_{O_2} = {iA}/{Fz} \quad (3)$$

where F_{O2} represents the mole flow (mol/m^2s) of oxygen, i is the current density (Am^{-2}), A is the active area of anode (m^2), F=96487 As/mol is the Faraday constant and z is the number of electrons involved

in the electrochemical reactions. In this case z=4, as can be derived from the equation relative to the anode (2).

Concerning the bubbles size, a dimension to numerically solve the problem needs to be prescribed *a priori*, since bubbles diameter is a required input. As a first approximation, the bubbles diameter was kept constant at 0.1 mm (100 μm). The chosen size comes from an approximated average of the measurements reported by Hreiz et al. [4], according to whom the bubble diameter grows with the vertical coordinate y, being about 60 μm at y=5 mm, and increasing to an average value near 120 μm from y=15 mm.

4.5. Interfacial forces

The force which mostly influences the motion of the bubbles inside the cell is the buoyancy force, due to the high difference of density between the electrolyte and the oxygen, respectively 1020 kg/m³ and 1.30 kg/m³. Between gas and liquid phases some interfacial forces occur which can be implemented inside Fluent®:

- drag force;
- lift force;
- wall lubrication force;
- virtual-mass force.

Drag force is highly influential in this kind of systems; among its expressions in the current study, three of them have been considered: Schiller-Naumann, Morsi-Alexander and Ishii-Zuber. The first two cited forces consider a rigid, spherical shape of the bubbles, coherently with our test case. In fact, the visualization of the flow in [4] shows that the bubbles are not deformed (Figure 2). On the other hand, the formulation of Ishii-Zuber is completer and more suitable for a boiling flow like the one studied. Having conducted simulations with the three forms of drag force without significant difference in the output, the choice has finally fallen on the Ishii-Zuber expression. To enable the use of this model, it is necessary to indicate the surface tension, considered equal to the one of water at room temperature, 72 mN/m.

Coming to the lift force, the solver's guidelines suggest that its inclusion can be helpful when having large bubbles [12]. As a matter of fact, such force is driven by a difference of pressure on the sides of the bubbles, due to a difference of velocity in the flow, according to Bernoulli's equation. Since in our case only small bubbles have been considered, lift force can be neglected so as not to put extra complications to the system.

The wall lubrication force pushes the secondary phases away from walls, acting in the normal direction. Such force was added to the model to improve the prediction of gaseous phase volume fraction profiles in the regions close to the electrodes. Among the possible models, Tomiyama and Frank ones are suitable for flows inside pipes [12], whereas Hosokawa takes by default the wall lubrication coefficient of Tomiyama and its manual characterization is not straightforward and adds complexity to the model. On the other hand, the study case is not a pipe flow, thus the only possible choice was the Antal formulation. Wall lubrication coefficients *Cw1* and *Cw2* default values, namely -0.01 and 0.05, were used.

As for virtual-mass force, in biphasic flows a "virtual-mass effect" occurs when the secondary phase accelerates relative to the primary phase. It is a relevant force when the difference of densities between the phases is high, and such it is in the case study. A constant coefficient of 0.5 was chosen to simplify the CFD code, corresponding to spherical shape of bubbles.

5. Results and discussion

5.1. Y-velocity field

To evaluate the accuracy of the model described, the main parameter considered was the mean bubbles y-velocity field in the mid-section, that is the velocity of the gas flow in the vertical direction. This output was compared with the gas velocity fields that Hreiz et al. [4] were able to obtain by use of a PIV algorithm. Three different cases of current density have been studied: Figures 3, 4 and 5 show the velocity fields with current densities 65, 130 and 260 Am^{-2}, respectively.

Qualitatively speaking, the bubbles curtain with growing thickness was reproduced numerically. However, the gas spreading to the central part of the cell is less evident than the experimental measurements. Quantitatively speaking, instead, the maximum values of velocity are close to the ones obtained experimentally. The applied current densities of 65, 130 and 260 Am^{-2} gave maximum y-velocities of 16, 22, 29 mm/s, respectively. These numbers are consistent with the ones obtained by Hreiz et al. with PIV [4] apart from the third case (260 Am^{-2}) with higher velocities than PIV results.

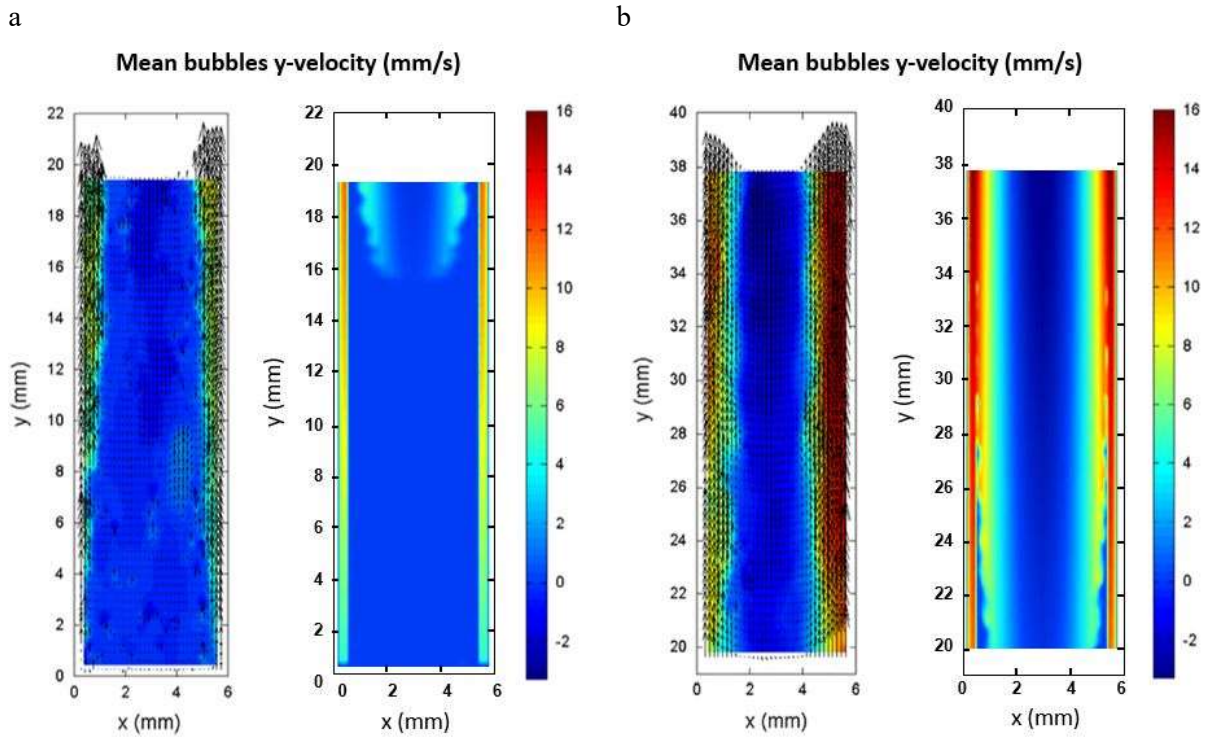

Figure 3. Mean y-velocity contour plots: on the left PIV output [4], on the right numerical results, 65 Am^{-2}. (a) Bottom half of the cell, for $0 \leq y \leq 19$ mm. (b) Top half of the cell, for $19 \leq y \leq 38$ mm

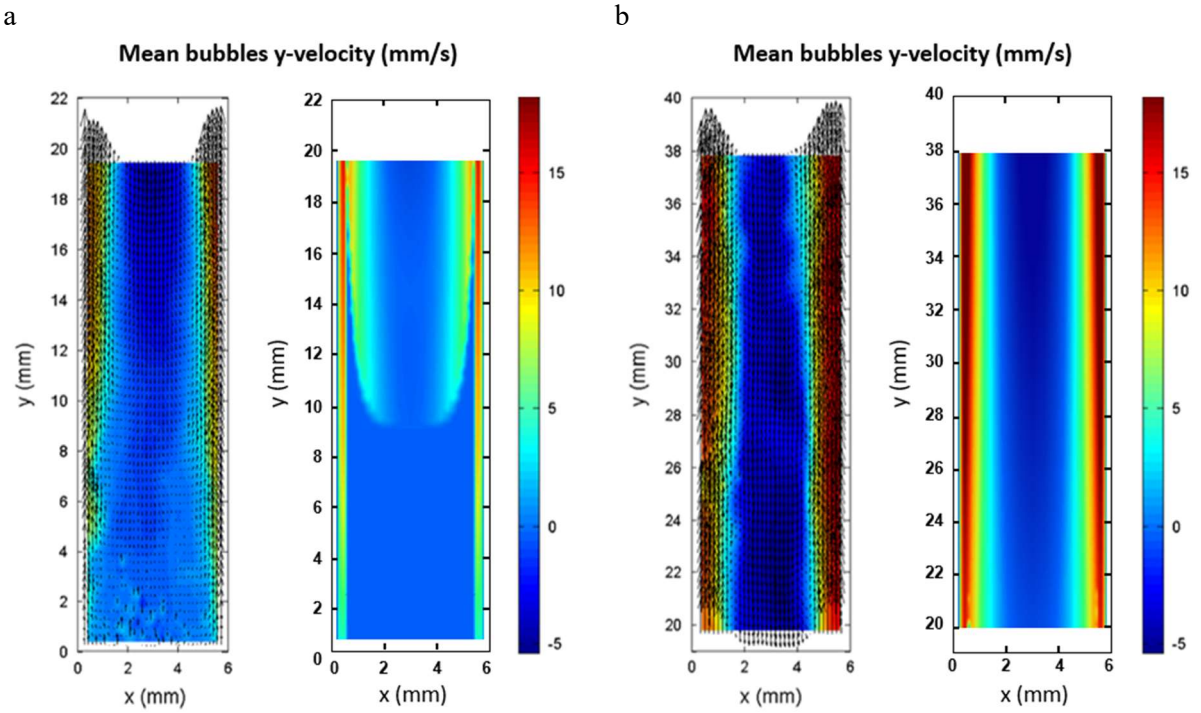

Figure 4. Mean y-velocity contour plots: on the left PIV output [4], on the right numerical results, 130 Am^{-2}. (a) Bottom half of the cell, for $0 \leq y \leq 19$ mm. (b) Top half of the cell, for $19 \leq y \leq 38$ mm

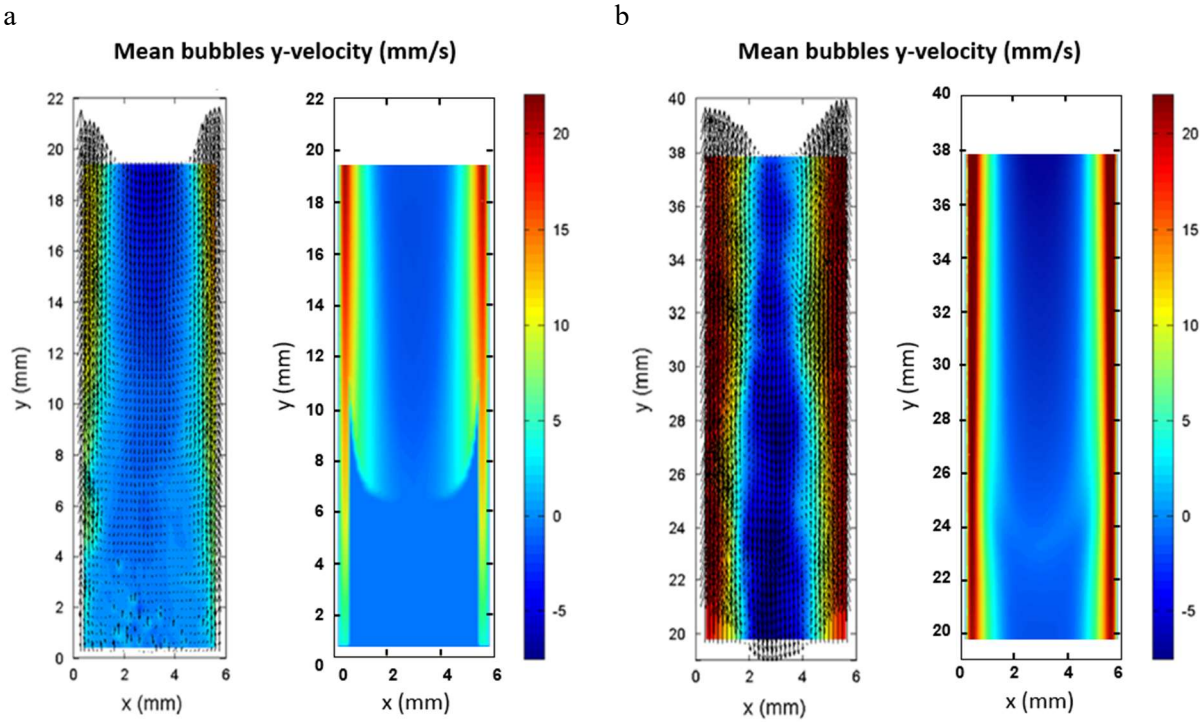

Figure 5. Mean y-velocity contour plots: on the left PIV output [4], on the right numerical results, 260 Am^{-2}. (a) Bottom half of the cell, for $0 \leq y \leq 19$ mm. (b) Top half of the cell, for $19 \leq y \leq 38$ mm

5.2. Source layer thickness

A dedicated sensitivity analysis was performed to assess the size of the layer where the mass source term is introduced. Thus, four different cases of geometry were studied with fixed current density of 130 Am^{-2}, namely 0.1 mm, 0.2 mm, 0.4 mm and 0.8 mm of source layer thickness. Figure 6 shows the results for the y-velocity field of all the computational domain. The first case looks more unstable than the other ones with more frequent vortices inside the gas flow. Furthermore, the bubble curtain reaches lower y-velocities when compared to the experimental measurements in Figure 4. Finally, the negative velocities of the recirculating electrolyte solution are not as high as they are expected to be. Thus, the 0.1 mm layer thickness is to be excluded. A better behaviour is shown by the 0.2 mm case. However, when considering the recirculation pattern of the flow in the bottom half of the cell, it seems not as strong as for PIV results displayed in Figure 4a, with the downward flow stopping at a 15 mm height instead of reaching lower y values. From this point of view, the 0.4 and 0.8 mm cases seem to perform better. However, the last case shows a worse correspondence with the measurements in the upper part of the cell, where the gas curtain seems to shrink instead of thickening. Hence, also the 0.8 mm case was considered not matching with experiments and the 0.4 mm case confirmed its validity.

This analysis provides an idea about the importance of choosing the geometry of the source layer.

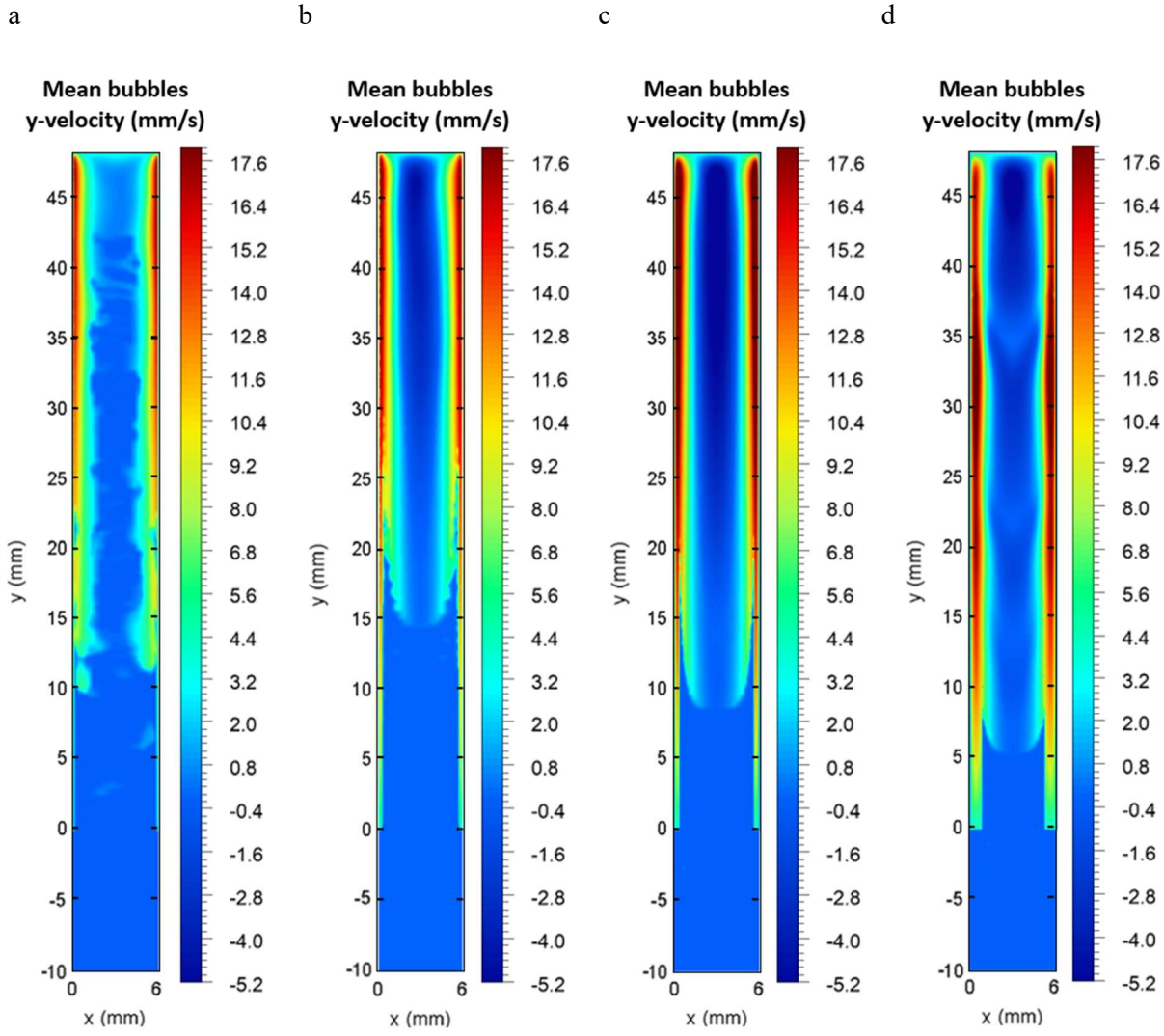

Figure 6. Contour plot of the mean bubbles y-velocity in the reactor mid-plane. Source layer thickness: (a) 0.1 mm, (b), 0.2 mm, (c) 0.4 mm, (d) 0.8 mm

5.3. Bubbles dimension

The impact of varying the bubble size was also analysed for the 130 Am^{-2} condition. First, two bubbles diameters were imposed and studied, namely 60 and 75 µm, both smaller than the average measured diameter of 100 µm. The cited diameter cases showed a flow behaviour with recirculating cells of length proportional to the bubble size: shorter cells, corresponding to six vortices, occur in the 60 µm case (Figure 7a), three vortices are present in the 75 µm case (Figure 7b) while only one longer recirculating cell occurs in the 100 µm case (Figure 7c). Such a hydrodynamic phenomenon can be explained when analysing the maximum y-velocity for the cited bubbles diameters: velocities of 15, 18 and 22 mm/s can be observed for the cases with 60, 75 and 100 µm bubbles diameters, respectively. As expected, due to the buoyancy force, higher velocities are related to a larger bubbles size. At the same time, lower velocities may cause a more frequent occurrence of recirculating flows.

The impact of bigger bubbles on the solution was then evaluated, changing the diameter from 100 µm to 150 µm. The influence of the so called Very Large Bubbles (VLBs), about 1 mm large, is thought to be crucial in the spreading of the gas curtain towards the inner part of the cell [4]. On the other hand, flow visualization shows that VLBs are not frequent (as in Figure 2), thus the diameter was just increased of a 50 % with respect to the model default, although leading to a bubble volume 3.3 times bigger. As a matter of fact, the model built so far is only able to introduce a uniform shape of bubbles. The output is shown in Figure 7d, where it is compared to the other diameter cases. It is possible to see that, on one side, a bigger bubble diameter allows us to better simulate the gas spreading and thickening of the bubbles curtain in the vertical direction, whereas, on the other side, it is not able to reproduce a suitable recirculation pattern, as it was shown in the PIV measurements.

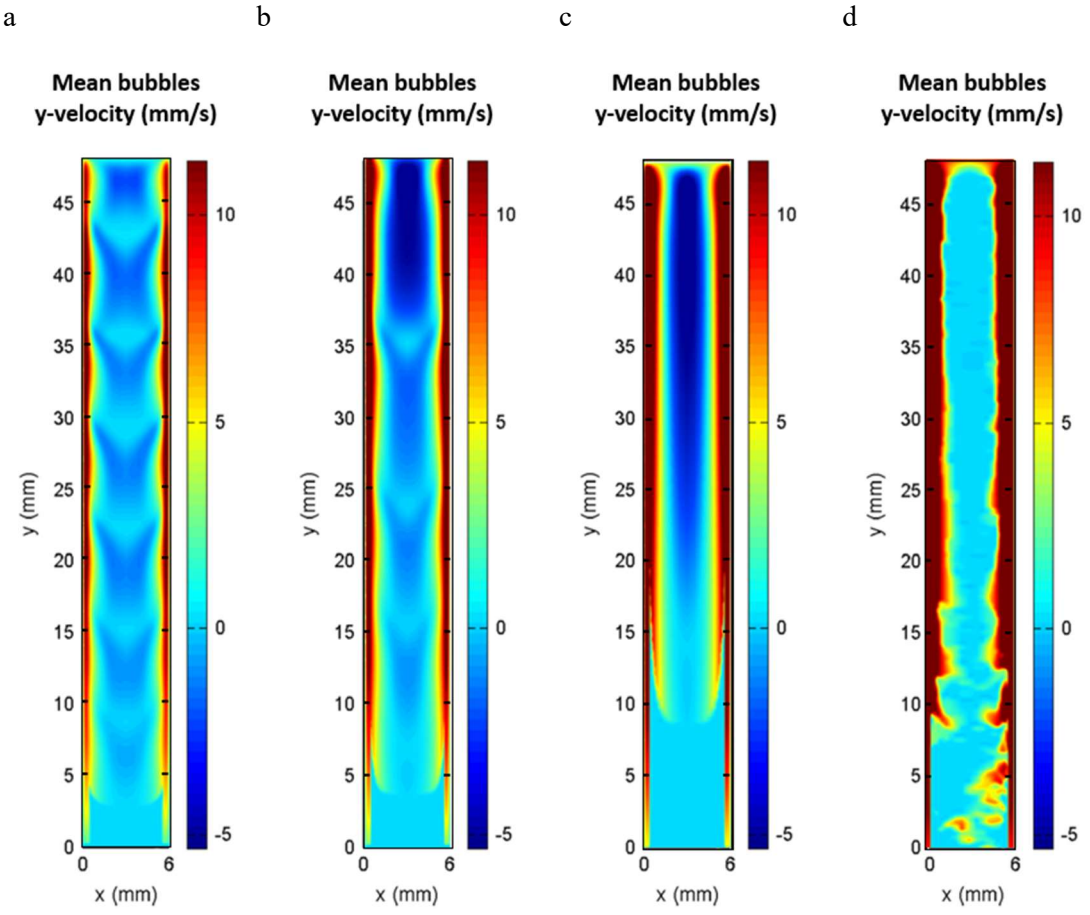

Figure 7. Contour plot of the mean bubbles y-velocity in the reactor mid-plane. Bubbles diameter: (a) 60 µm, (b) 75 µm, (c) 100 µm, (d) 150 µm

In conclusion, the 100 μm-diameter case represents the best trade-off for the present model, allowing a gas diffusion and a downward recirculation consistent with experimental results. As a matter of fact, this value is in-line with the measurements of the bubble diameter, as described above.

6. Conclusions

The study presents an accuracy assessment of the Eulerian CFD modelling for an electrochemical cell. A literature review was conducted, showing that no consensus is present about the most suitable numerical model for this kind of simulations. A case study of a No Net Flow cell was taken as reference to evaluate the numerical results. The chosen model and sub-models are thoroughly described and validated with experimental data; in particular, the CFD solution was compared to PIV measurements of the vertical mean velocity of the generated gas, showing good agreement in maximum values, for three conditions in terms of current density. However, qualitatively speaking, the thickening of the bubbles curtain is slightly underestimated and the model needs further refinement.

The impact of the source layer size was studied, considering four different cases of thickness, namely 0.1, 0.2, 0.4 and 0.8 mm. The conclusion of this analysis is that the definition of the source layer size is crucial and needs to be calibrated depending on the expected gas volume fraction. A comparison with the experimental results confirmed the layer thickness of 0.4 mm for the present model.

The influence of the bubble dimension on the model was then evaluated. In addition to the 100 μm-diameter case, two smaller and a larger diameter were evaluated, namely 60, 75 and 150 μm. A growing number of recirculating cells was noticed as the bubble diameter decreases, likely due to the lower velocities of the gas. The bigger size of the bubbles showed instead a noticeable influence with respect to the diffusion of the gas towards the inner part of the cell. On the other hand, downward velocities differed from experimental measurements and the 100 μm-diameter case was assessed to be the most consistent with PIV results.

In conclusion, the present CFD model showed good agreement with the experimental test case. However, a refinement in the source term introduction is to be looked for in the future, especially concerning the non-uniformity of the bubble dimension, which is thought to be of major importance for the biphasic flow inside the cell. Furthermore, dispersion forces will be included in the model to assess their impact on the gas diffusion.

7. References

[1] Mayyas A, Wei M and Levis G, Hydrogen as a long-term, large-scale energy storage solution when coupled with renewable energy sources or grids with dynamic electricity pricing schemes, 2020, *International Journal of Hydrogen Energy* **45,** 16311–25.

[2] IEA, The future of hydrogen, 2019, https://www.iea.org/reports/the-future-of-hydrogen.

[3] Ulleberg Ø, Modeling of advanced alkaline electrolyzers: a system simulation approach, 2003, *International Journal of Hydrogen Energy* **28**, Issue 1, 21–33.

[4] Hreiz R, Abdelouahed L, Fuenfschilling D, and Lapicque F, Electrogenerated bubbles induced convection in narrow vertical cells: PIV measurements and Euler–Lagrange CFD simulation, 2015, *Chemical Engineering Science* **134**, 138–152.

[5] Le Bideau D, Mandin P, Benbouzid M, Kim M, Sellier M, Ganci F and Inguanta R. Eulerian Two-Fluid Model of Alkaline Water Electrolysis for Hydrogen Production, 2020, *Energies* **13**, 3394.

[6] Abdelouahed L, Hreiz R, Poncin S, Valentin G and Lapicque F, Hydrodynamics of gas bubbles in the gap of lantern blade electrodes without forced flow of electrolyte: Experiments and cfd modelling, 2014a, *Chem. Eng. Sci.* **111**, 255–265.

[7] Zarghami A, Deen N G and Vreman A W, CFD modeling of multiphase flow in an alkaline water electrolyzer, 2020, *Chemical Engineering Science* **227** 115926.

[8] El-Askary W, Sakr I, Ibrahim K and Balabel A, Hydrodynamics characteristics of hydrogen evolution process through electrolysis: Numerical and experimental studies, 2015, *Energy* **90**, 722–737.
[9] Mat M D, Aldas K, Ilegbusi O J, A two-phase flow model for hydrogen evolution in an electrochemical cell, 2004, *International Journal of Hydrogen Energy* **29**, Issue 10, 1015-23,
[10] Tijani A S, Yusup N A B and Rahim A H A, Mathematical Modelling and Simulation Analysis of Advanced Alkaline Electrolyzer System for Hydrogen Production, 2014, *Procedia Technology* **15**, 798–806.
[11] Shen M, Bennett N, Ding Y and Scott K, A concise model for evaluating water electrolysis, 2011, *International Journal of Hydrogen Energy* **36** Issue 22, 14335–41.
[12] *ANSYS Fluent Theory Guide*, 2020.